JACS
JOURNAL OF THE AMERICAN CHEMICAL SOCIETY

Article

pubs.acs.org/JACS

Molecular Catch Bonds and the Anti-Hammond Effect in Polymer Mechanochemistry

Sai Sriharsha M. Konda,[†,§] Johnathan N. Brantley,[†,§] Bibin T. Varghese,[†] Kelly M. Wiggins,[†] Christopher W. Bielawski,*[,†] and Dmitrii E. Makarov*[,†,‡]

[†]Department of Chemistry and Biochemistry, University of Texas at Austin, Austin, Texas 78712, United States
[‡]Institute for Computational Engineering and Sciences, University of Texas at Austin, Austin, Texas 78712, United States

Supporting Information

ABSTRACT: While the field of polymer mechanochemistry has traditionally focused on the use of mechanical forces to accelerate chemical processes, theoretical considerations predict an underexplored alternative: the suppression of reactivity through mechanical perturbation. Here, we use electronic structure calculations to analyze the mechanical reactivity of six mechanophores, or chemical functionalities that respond to mechanical stress in a controlled manner. Our computational results indicate that appropriately directed tensile forces could attenuate (as opposed to facilitate) mechanochemical phenomena. Accompanying experimental studies supported the theoretical predictions and demonstrated that relatively simple computational models may be used to design new classes of mechanically responsive materials. In addition, our computational studies and theoretical considerations revealed the prevalence of the anti-Hammond (as opposed to Hammond) effect (i.e., the increased structural dissimilarity between the reactant and transition state upon lowering of the reaction barrier) in the mechanical activation of polyatomic molecules.

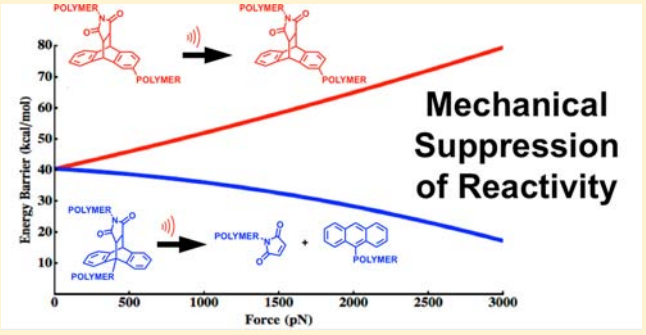

INTRODUCTION

The use of mechanical forces to bias chemical reactions, commonly referred to as mechanochemistry,[1] has increasingly found applications in the synthetic and materials science communities. Within this field, polymer mechanochemistry, or the mechanical manipulation of reactive functional groups (termed mechanophores) embedded within polymeric matrices, has attracted considerable attention due to its ability to facilitate a number of otherwise kinetically inaccessible processes.[2] While theoretical models have been shown to successfully account for these experimental observations,[3] such models are typically used as postexperimental rationalizations. Here, we show that theoretical analysis may be used to guide the rational design of mechanophores that exhibit novel, force induced reactivity. Moreover, our results uncovered general trends in the mechanical response of polyatomic molecules that have significant implications for the design of new mechanophores and force responsive materials. These trends stem from the inherent multidimensionality of mechanochemical processes and, therefore, cannot be accounted for by one-dimensional models commonly used to explain mechanical activation.[4] Indeed, while the one-dimensional approximation necessitates that force acts in the direction of the reaction coordinate (RC), thereby lowering the transition state (TS) barrier and accelerating the associated transformation, we will show that such an alignment between the force and a typical RC is extremely improbable in the high-dimensional configuration space of a typical mechanophore.

THEORETICAL DISCUSSION

Misalignment between mechanical stress and the targeted reaction pathway can result in a number of distinct scenarios. Figure 1 illustrates some of these activation motifs using a model two-dimensional potential energy surface (PES) that exhibits a single minimum (which corresponds to the reactant) and a saddle-point (which corresponds to the TS). Of the two coordinates that specify the molecular configuration, R quantifies the mechanical strain (which, in most experimental studies, corresponds to the distance between a pair of atoms on which the applied force is exerted), and X represents the remaining molecular degrees of freedom. While similar scenarios to those depicted in Figure 1 have been explored,[5] we emphasize that the reduction to two degrees of freedom is an oversimplification in the present context and is only used for illustrative purposes.

A force F acting along the mechanical coordinate R performs mechanical work ($W = F\Delta R$) as the molecule evolves toward the TS, where ΔR is the change in the mechanical pulling coordinate. The activation energy is effectively lowered by W and the transition rate $k(F)$ is enhanced by a factor of e^{W/k_BT} =

Received: May 21, 2013
Published: August 2, 2013

   dx.doi.org/10.1021/ja4051108 | J. Am. Chem. Soc. 2013, 135, 12722−12729

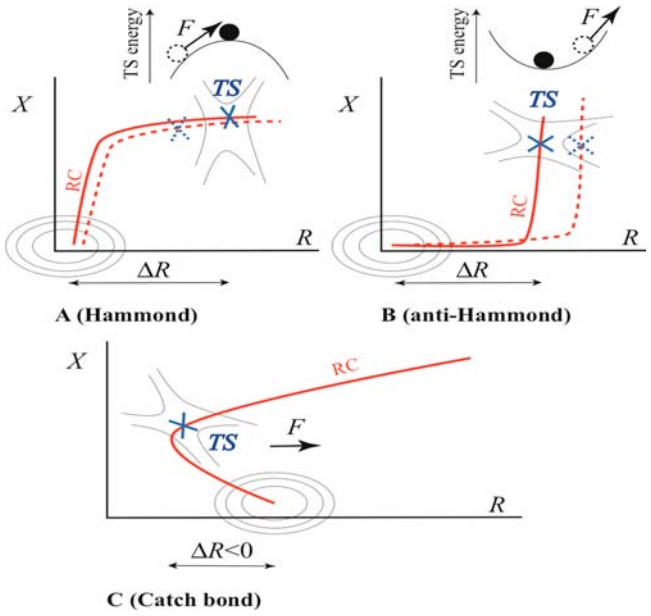

Figure 1. Force induced changes on a reaction pathway. (A) The Hammond effect, where the "true" reaction coordinate (RC, red line) is aligned with the mechanical coordinate (R). Mechanical equilibrium necessitates that a pulling force (F) shifts the TS toward the reactant state minimum (because the TS energy exhibits a maximum along R). The shifted RC and the new TS are shown as a dashed red line and a blue "×", respectively. (B) The anti-Hammond effect, where there is misalignment between RC and R (so that the TS exhibits a minimum as a function of R) and the TS is more compliant than the reactant. (C) Catch bond behavior, where molecular distortion along R initially decreases but later increases along the RC.

$e^{F\Delta R/k_BT}$. This result, commonly referred to in the literature as the "Bell formula",[4] however, does not account for the force induced displacement of the reactant and transition states. If the true RC (i.e., the steepest descent path connecting the TS saddle point to the reactant state minimum on the PES) coincides with the mechanical coordinate (Figure 1A), then a stretching force pushes the TS toward the reactant. This phenomenon is usually referred to as the Hammond effect, which posits that the reactant and TS structures are driven toward each other as the barrier separating them is lowered.[3a,6] As the Hammond effect reduces the molecular distortion (i.e.,ΔR), it weakens the force dependence of the reaction rate.

A very different scenario is shown in Figure 1B, where the mechanical coordinate is misaligned with the RC in the vicinity of the TS saddle such that the TS energy exhibits a minimum (rather than a maximum) when R is varied. Consequently, a pulling force F may increase the separation between the TS and the reactant, thus resulting in "anti-Hammond" behavior. In this case, the structural separation between the reactant and the TS increases, but the energy barrier between these two states decreases. As the anti-Hammond effect increases the work done by the force, it provides an additional acceleration of the reaction rate.

These considerations are quantified in the recently reported Extended Bell Theory (EBT),[3c−e] which accounts for the force induced shifts of the TS and reactant states along a given reaction pathway in the 3N-dimensional (where N is the number of atoms) configuration space of the molecular system of interest. To second-order in the applied force, the reaction rate $k(F)$ is given by[3d]

$$\ln k(F)/k(0) \approx (k_BT)^{-1}(F\Delta R + F^2\Delta\chi/2) \quad (1)$$

The $F\Delta R$ term in eq 1 is identical to Bell's formula. The quadratic term results from the interplay of two effects: (1) the elastic energy stored in the molecule as a result of mechanical deformation and (2) the additional work done by the applied force as a result of the Hammond or anti-Hammond shift in ΔR. This shift is described by the formula

$$\Delta\Delta R = \Delta R_{TS} - \Delta R_r = \chi_{TS}F - \chi_rF = \Delta\chi F \quad (2)$$

where χ_r and χ_{TS} are, respectively, the compliances of the reactant state and TS in response to pulling along R. These compliances can be computed from the molecule's $(3N \times 3N)$ Hessians in the reactant and TS configurations[3d] as described below. A key departure from one-dimensional theories[4] is that the TS compliance (χ_{TS}) can be either positive or negative.[3d] As a result, both anti-Hammond ($\Delta R > 0$; $\Delta\chi > 0$) and Hammond ($\Delta R > 0$; $\Delta\chi < 0$) behavior is possible. We emphasize that the Hammond or anti-Hammond behavior is controlled by $\Delta\Delta R$, which is the shift in the reactant-to-TS distortion in response to the applied force.

COMPUTATIONAL RESULTS AND DISCUSSION

To explore the correlation between mechanical activation and the direction along which the pulling force is exerted, we have performed a comprehensive survey of all possible pulling scenarios in the context of six previously reported mechanically induced transformations: the conrotatory electrocyclic ring-opening of *cis*- and *trans*-disubstituted benzocyclobutene,[2a] the formal [3 + 2] cycloreversion of 1,2,3-triazoles,[2c,e] the formal [4 + 2] cycloreversions of a furan/maleimide Diels−Alder adduct and a maleimide/anthracene Diels−Alder adduct,[2f] and the isomerization of a spiropyran derivative[2g] (Scheme 1).

Scheme 1. Mechanophore Models

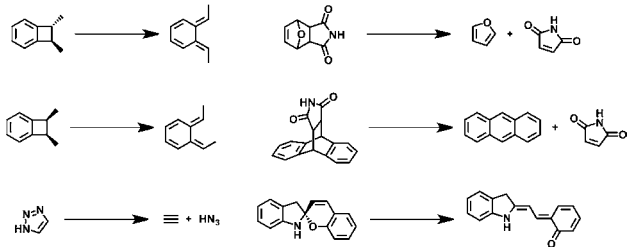

In order to probe the intrinsic reactivity of each mechanophore in the absence of strongly perturbing steric or electronic environments, we employed truncated analogues bearing only hydrogen substituents (although methyl substituents were used to account for stereochemistry when necessary). For the same reason, polymeric handles, while important,[3g,7a] were not included in the calculations. In other words, the force appearing in eq 1 is assumed to be exerted directly on a pair of atoms belonging to the mechanophore. The mechanism through which the force is transmitted to the mechanophore and its dependence on, e.g., experimental design or the structure of the polymer backbone, is not considered here. Instead, we sought to demonstrate that the qualitative trends one obtains from our simplified model can aid in the experimental design of new systems (even though some pulling scenarios are strictly "thought" experiments).

dx.doi.org/10.1021/ja4051108 | J. Am. Chem. Soc. 2013, 135, 12722−12729

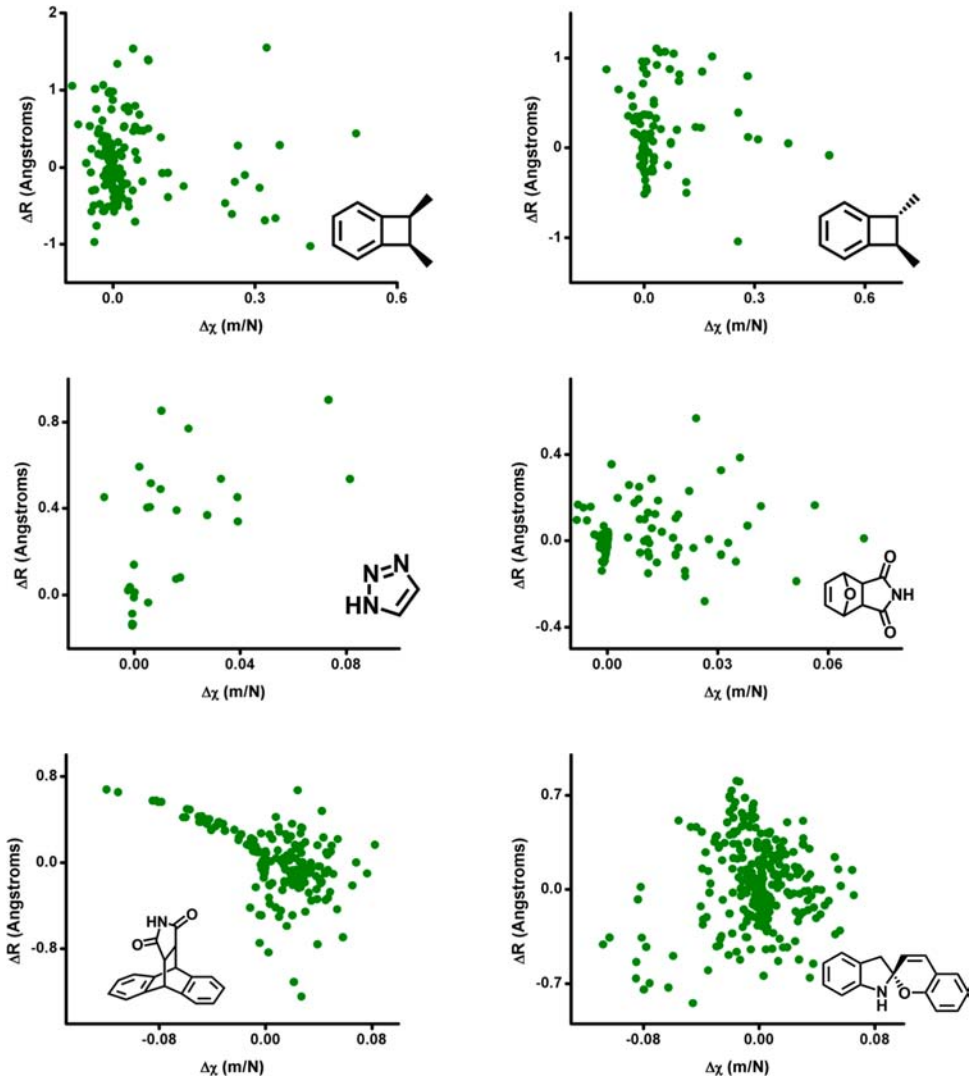

Figure 2. Computed values of ΔR and $\Delta\chi$ for all possible combinations of pulling points for the indicated mechanophores. Nearly all combinations result in a positive value of $\Delta\chi$; however, both signs of ΔR are present with almost equal frequency.

EBT calculations were performed with the NWCHEM package[8] using density functional theory,[9] employing the 6-31G* basis set[10] and the B3LYP exchange-correlation energy functional.[11a] To verify the insensitivity of our results to the choice of the density functional and the basis set, we also repeated calculations using the M05-2X hybrid meta exchange-correlation functional[11b] and the 6-31++G**/6-31G* basis sets (see the SI for details). The nature of the stationary points was confirmed by a vibrational frequency analysis. In addition, each TS was confirmed by following the reaction coordinate from the TS to the reactant and the product using the intrinsic reaction coordinate (IRC) method.[12,13] The force dependence of the reaction rate was estimated using eq 1, where $\Delta R = R_{TS} - R_r$ was computed from optimized reactant and TS geometries. To compute $\Delta\chi = \chi_{TS} - \chi_r$, we used the identity[3d] $\chi_{r,TS} = 2/\lambda$, where λ is the nonzero eigenvalue of the 6×6 matrix

$$\bar{\mathbf{h}}_{11} = \mathbf{h}_{11} - \mathbf{h}_{12}(\mathbf{h}_{22})^{-1}\mathbf{h}_{21} \tag{3}$$

computed, respectively, from the reactant or TS Hessian matrix

$$\mathbf{h} = \begin{pmatrix} \mathbf{h}_{11} & \mathbf{h}_{12} \\ \mathbf{h}_{21} & \mathbf{h}_{22} \end{pmatrix} \tag{4}$$

In eq 4, this matrix is written in block form in terms of, respectively, 6×6, $6 \times (3N - 6)$, $(3N - 6) \times 6$, and $(3N - 6) \times (3N - 6)$ matrices $\mathbf{h}_{11}$, $\mathbf{h}_{12}$, $\mathbf{h}_{21}$, and $\mathbf{h}_{22}$.[3d] Equation 4 further assumes that the atoms are renumbered such that one always pulls on atoms 1 and 2. In contrast to the experimental and earlier computational studies, we evaluated all $N(N - 1)/2$ possible pulling points for each mechanophore scaffold of N atoms, which resulted in a total of 1456 simulated pulling experiments. The use of the EBT approximation allows one to accomplish this seemingly formidable task at modest computational expense.

We systematically determined $\Delta\chi$ (i.e., $\chi_{TS} - \chi_r$) and ΔR (i.e., $R_{TS} - R_r$) for each atom pair, and the corresponding results are summarized in Figure 2. Surprisingly, a comparable number of instances of reaction suppression ($\Delta R < 0$) and enhancement ($\Delta R > 0$) were observed. This finding is counterintuitive, as is apparent from the thought experiment involving the application of forces to the two atoms belonging to a diatomic molecule. Suppressing bond scission would

dx.doi.org/10.1021/ja4051108 | J. Am. Chem. Soc. 2013, 135, 12722−12729

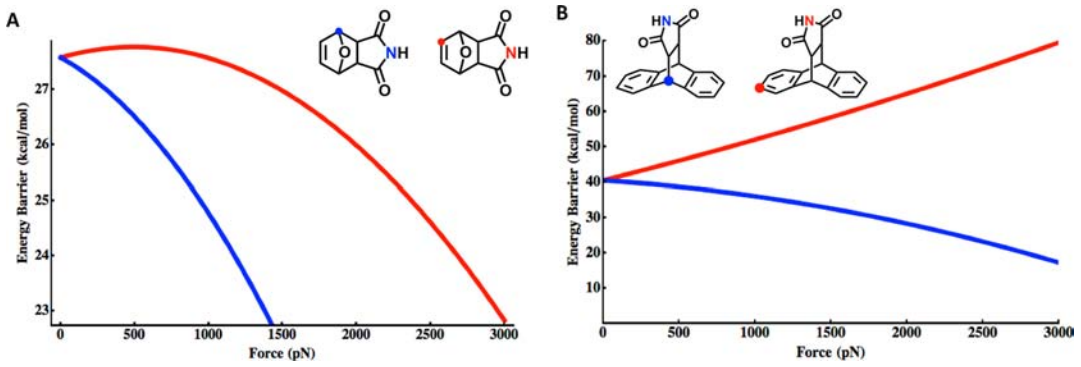

Figure 3. Examples of mechanically accelerated and mechanically suppressed reactivity. (A) Computed changes in the activation energy (equal to $U_{TS} - U_R - F\Delta R$, where $U_{r(TS)}$ is the reactant (or TS) energy on the force-modified potential energy surface) for the cycloreversion of a Diels–Alder adduct using pulling points for reaction acceleration (blue) and pulling points for reaction suppression (red). Note the rollover behavior: a catch bond at low forces is superseded by a slip bond at a higher force. (B) Computed changes in the activation energy for the cycloreversion of a Diels–Alder adduct using the pulling points for reaction acceleration (blue) and the pulling points for reaction suppression (red).

require that the forces push the atoms toward each other, but such an arrangement of atoms leads to mechanical instability akin to that experienced by a pencil balanced on its tip. Direct bond compression, therefore, cannot account for reaction suppression, which, instead, must require an indirect mechanism involving coupled distortions of multiple bonds. A cartoon depiction of this suppression mechanism is given in Figure 1C, where an RC in the multidimensional configuration space diverges from the mechanical coordinate such that the stretching force pushes the molecule away from its energetically favorable pathway.

A similar phenomenon has been observed for the forced dissociation of biomolecular adhesion complexes,[14] where mechanical suppression of dissociation is known as the "catch bond" or "molecular jamming" effect.[15] While theoretically predicted,[3c,f,5] catch bonds are fairly atypical; conversely, "slip bonds", whose dissociation is promoted by force, are more common.[16] Only recently have catch bond effects (i.e., the apparent strengthening of a covalent bond under mechanical stress) been described in mechanochemical transformations involving nonbiological chemical systems. In particular, Boulatov and colleagues reported the kinetic stabilization of esters toward hydrolysis under tension,[17a] and Marx et al. showed that disulfide bonds are less susceptible to nucleophilic attack under the action of mechanical force.[17b] Our results, however, suggest that catch bonds may be common in a variety of chemical transformations. A few salient examples are presented in Figure 3, which show that even a subtle change in mechanophore design may result in a switch from slip bond to catch bond behavior. Moreover, a "rollover" phenomenon similar to that predicted for biomolecular catch bonds[3f,5] is observed (i.e., a catch bond at low forces that becomes superseded by a slip bond at higher forces; for further details, see Supporting Information Figures S3–S5 and Videos S1–S2). The ability to selectively suppress a chemical transformation through the application of mechanical stress could have important design implications, particularly in the context of molecular machines or force responsive materials.[18] For example, mechanical degradation of such systems could be attenuated by directing external loads to mechanically labile bonds in a manner that would suppress bond scission. Furthermore, catch bond effects could potentially be harnessed to access materials that become more mechanically robust under stress.

A separate but equally intriguing trend observed in Figure 2 is the predominantly positive sign of $\Delta\chi$, which underscores the prevalence of the anti-Hammond effect in this study. While puzzling at first glance, this result stems from the multidimensional character of the underlying PES. A negative sign for the TS compliance (χ_{TS}), which would lead to a negative $\Delta\chi$, becomes statistically unlikely for systems of high dimensionality. Indeed, as shown in Figure 1A, χ_{TS} is negative only when the RC is sufficiently aligned with the mechanical coordinate R such that strain causes the TS energy to decrease. Since the TS configuration corresponds to a first-order saddle, there is only one normal mode along which the energy decreases, while there are $3N - 1$ modes along which the energy increases (or remains constant). Thus, the probability of favorable alignment between R and the RC becomes vanishingly small with increasing number of atoms, N. If, for example, the pulling direction is a random vector in the $3N$-dimensional space, then this probability is shown (Supporting Information) to decrease exponentially with N, thereby rendering a negative value of χ_{TS} highly improbable even for systems of modest size. Indeed, for all cases displayed in Figure 2, χ_{TS} was found to have a positive value (Supporting Information Figure S2). Note, however, that symmetry requirements may lead to perfect alignment between R and RC in certain pulling arrangements. Such cases would be exceptions to the trend observed here.

Of course, a positive sign for χ_{TS} does not guarantee anti-Hammond behavior, since $\Delta\chi$ could still be negative if $\chi_{TS} < \chi_r$. This scenario, while explaining the few instances of negative $\Delta\chi$ observed in Figure 2, should be rare, considering that the TS of a reaction involving bond scission is expected to be more mechanically labile than the relatively stable reactant state.

Although our findings are based on calculations that employ the EBT approximation (whose limitations have been discussed in the literature[3c,d,7b]), the above general considerations indicate that our conclusions are, in fact, not critically dependent on the underlying EBT assumptions. For example, recent studies[7a,b] highlight the effect of the statistical mechanical properties of the polymer backbone attached to the mechanophore on the overall mechanochemical reactivity. It would appear that multiple polymer conformations would invalidate the EBT assumption of a single TS. This situation is, however, common in condensed phase rate theory, where the assumption of a single PES saddle is inevitably incorrect. Coarse graining is the standard way of treating this problem,

dx.doi.org/10.1021/ja4051108 | J. Am. Chem. Soc. 2013, 135, 12722–12729

Scheme 2. Synthesis and Ultrasonication of Various [4 + 2] Cycloaddition Adducts[a]

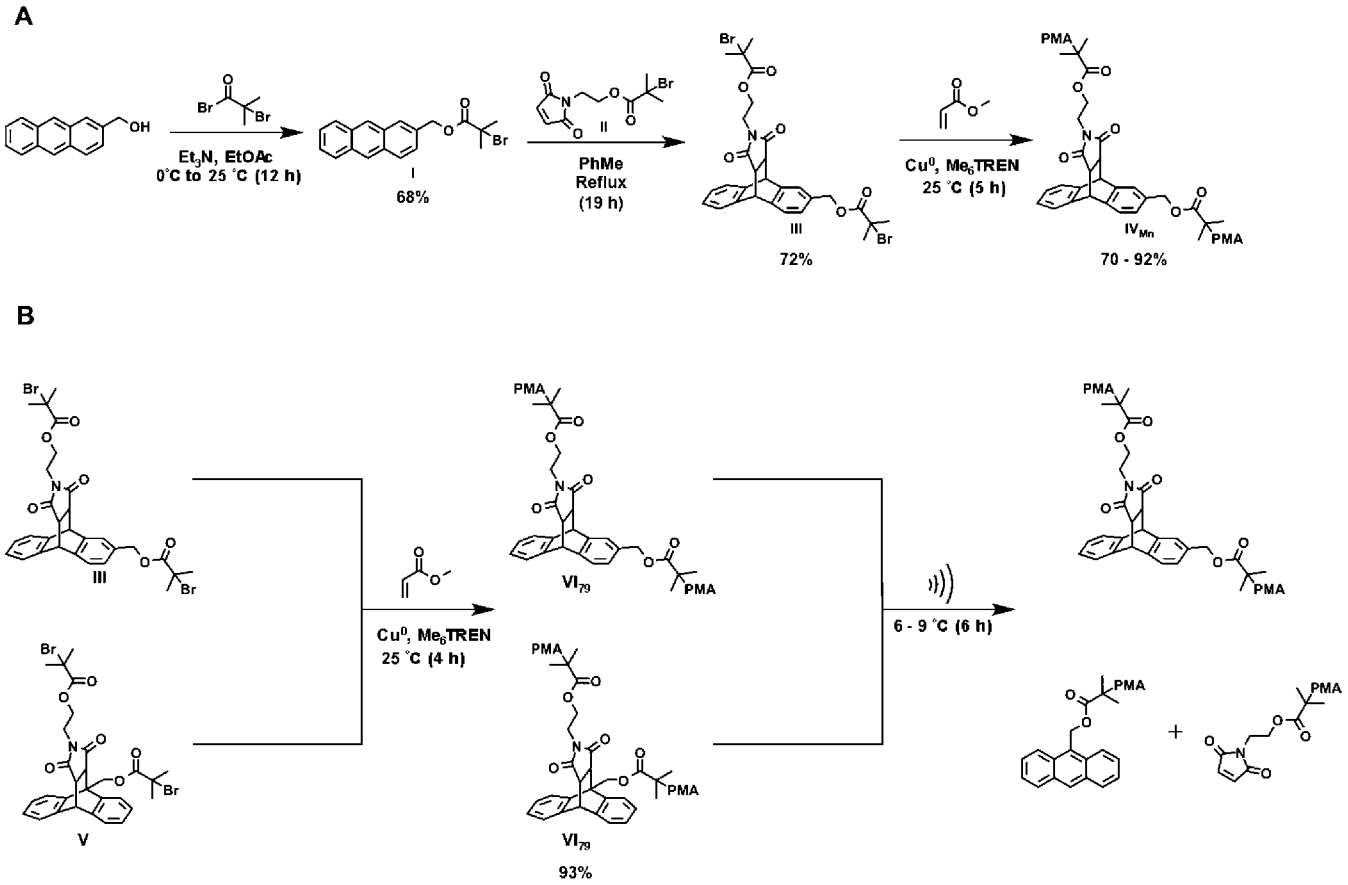

[a](A) Synthesis of a mechanophore predicted to exhibit mechanical suppression of reactivity. Me_6TREN = tris[2-(dimethylamino)ethyl]amine. Et_3N = triethylamine. PMA = poly(methyl acrylate). (B) Controlled radical polymerization of methyl acrylate from an equimolar mixture of the regioisomeric initiators **III** and **V** afforded a mixture of the associated PMA materials. Ultrasonication of the mixture resulted in the selective [4 + 2] cycloreversion of the adducts prepared from the 9-substituted anthracene derivatives.

where nonreactive degrees of freedom (such as those of the polymer backbone or a solvent) are removed; as a result, the PES becomes replaced by a (typically smoother) effective *free* energy surface (FES).[19a] Within this framework, the EBT formula 1 can be derived from Kramers' type theory or its multidimensional generalization due to Langer (see, e.g., the work of Hanggi et al.[19b]), provided that the extension ΔR is replaced by the *statistically averaged* extension and the susceptibilities χ_r and χ_{TS} are computed from the Hessian matrices of the FES.[20,5a] While the computation of a FES is a nontrivial task, the above arguments show that the anti-Hammond effect is not caused by some specific properties of the underlying PES but simply by its inherent multi-dimensionality. As such, this argument equally applies to any multidimensional FES. In support of this coarse-grained view of mechanochemical phenomena, studies of a two-dimensional FES led to the prediction of anti-Hammond behavior in force-induced protein unfolding,[5c] a finding supported by kinetic studies.[21]

EXPERIMENTAL METHODS AND DISCUSSION

To experimentally test the computational results and conclusions discussed above, subsequent efforts were focused on a system for which mechanical forces were predicted to suppress chemical reactivity. The Diels–Alder adduct derived from a 2-substituted anthracene moiety (c.f., the red pulling points in Figure 3B) was selected for our study for two reasons. First, our computational results predicted that a subtle change in mechanophore design (as compared to the originally reported system[2f]) would lead to a drastic change in reactivity. Moreover, this prediction appeared at variance with chemical intuition and thus provided a genuine example of designing a mechanophore from first-principles. Second, no rollover behavior was predicted in the force dependence of the reaction rate in this case (Figure 3B); thus, the predicted change in reactivity was expected to be observable under experimentally relevant conditions.

As shown in Scheme 2, the difunctional polymerization initiator **III** was prepared from the thermally promoted [4 + 2] cycloaddition between **I** (obtained from commercially available 2-anthracenyl methanol) and known[22a] maleimide derivative **II**. Subsequent Cu mediated controlled radical polymerization[22b] of methyl acrylate from **III** afforded chains of poly(methyl acrylate) (PMA) with varying number average molecular weights ($\mathbf{IV}_{Mn}$; M_n = 16, 56, 88, and 130 kDa; Supporting Information), depending on the $[\text{methyl acrylate}]_0/[\mathbf{III}]_0$. Initially, $\mathbf{IV}_{88}$ (M_n = 88 kDa; Đ = 1.3) was dissolved in acetonitrile (10 mg mL^{-1}) and subjected to pulsed ultrasound (1 s on; 1 s off; frequency = 20 kHz) for 5 h. Gel-permeation chromatography (GPC) revealed negligible changes in the M_n of the material isolated following acoustic treatment (c.f., M_n = 88 kDa vs M_n = 85 kDa for the presonicated and postsonicated

dx.doi.org/10.1021/ja4051108 | J. Am. Chem. Soc. 2013, 135, 12722–12729

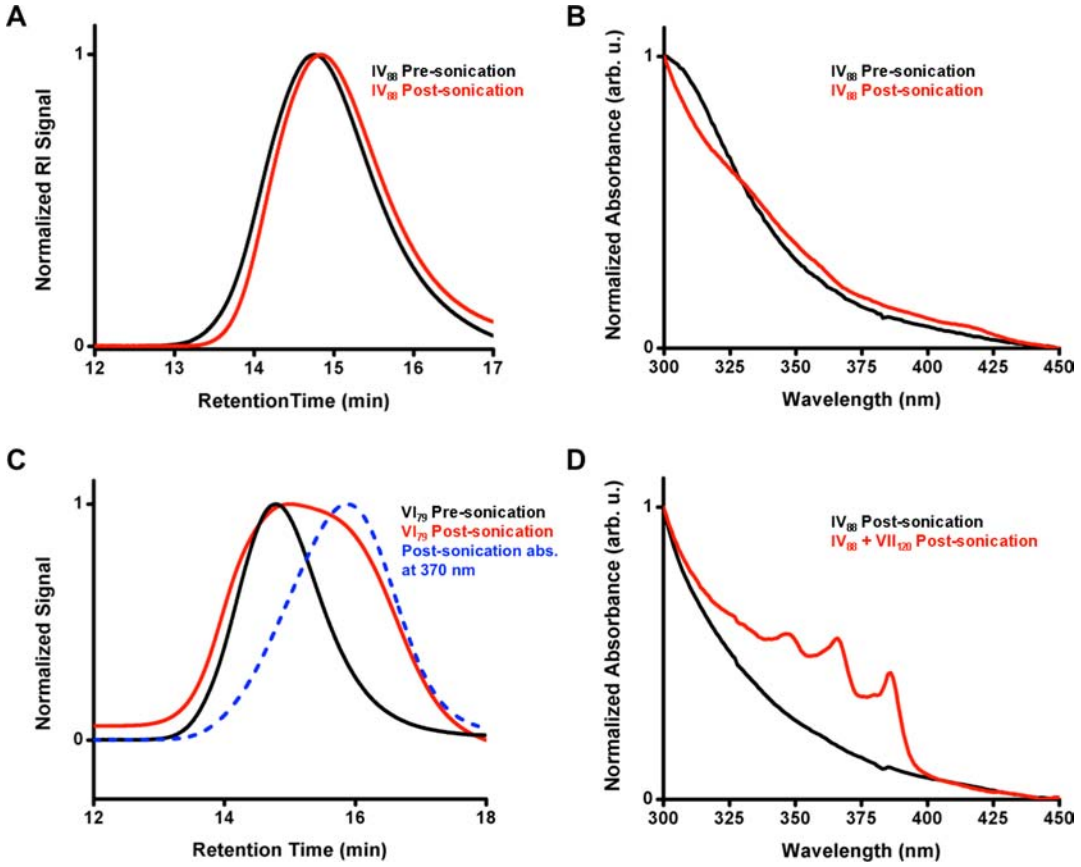

Figure 4. Experiments designed to verify the mechanical suppression of reactivity. (A) $\mathbf{IV}_{88}$ (black) exhibited minimal chain scission following ultrasonication (red). (B) The ultraviolet−visible absorption spectra of $\mathbf{IV}_{88}$ in THF (10 mg mL^{-1}) presonication (black) and postsonication (red). The absorbances characteristic of anthracene were not observed. (C) $\mathbf{VI}_{79}$ (i.e., the material prepared via polymerization of methyl acrylate from an equimolar mixture of **III** and **V**; black) exhibited chain scission following ultrasonication (red); however, the bimodal distribution of molecular weights was consistent with only some of the original polymer chains undergoing scission. Ultraviolet−visible detection at 370 nm (an absorbance wavelength of anthracene) reflected the generation of anthracenyl terminated polymers in the low molecular weight region of the bimodal distribution (Blue). (D) The ultraviolet−visible spectrum of $\mathbf{IV}_{88}$ in THF (10 mg mL^{-1}) was obtained postsonication (black). The absorbance characteristics of anthracene were not observed. $\mathbf{VII}_{120}$ was added to the postsonicated material, and the resulting mixture was resubjected to ultrasonication. The resulting material was isolated via precipitation from MeOH and dissolved in THF (10 mg mL^{-1}). Ultraviolet−visible absorption spectroscopy revealed the generation of the absorbances characteristic of anthracene (red).

materials, respectively; Figure 4A). Moreover, ultraviolet−visible spectroscopy revealed no change in the material's absorbance profile following ultrasonication (Figure 4B). As a mechanically induced cycloreversion would be expected to generate anthracenyl terminated polymer fragments (which would give rise to the detectable and characteristic absorbance profile of anthracene[2f]), the lack of anthracene absorbances was consistent with the conclusion that mechanical forces were not effecting a formal cycloreversion of the centrally located Diels−Alder adduct within $\mathbf{IV}_{88}$.[23] Similarly, ultrasonication of all the aforementioned $\mathbf{IV}_{Mn}$ polymers did not result in any detectable formation of anthracenyl terminated polymer fragments (as determined by GPC and ultraviolet−visible spectroscopy; Supporting Information). Moreover, the rate constants of chain scission for the $\mathbf{IV}_{Mn}$ polymers were found to be 2 orders of magnitude lower than those reported for the mechanically labile analogues embedded within polymers of similar molecular weight (c.f., $6.39 \times 10^{-5} \pm 3.42 \times 10^{-8}$ min^{-1} for $\mathbf{IV}_{88}$ vs $5.2 \times 10^{-3} \pm 0.1 \times 10^{-3}$ min^{-1} for the mechanically sensitive congener embedded in a PMA with an M_n of 71 kDa).[2f] Taken in combination with the lack of anthracene generation following ultrasonication, these data strongly indicated that the $\mathbf{IV}_{Mn}$ polymers were resistant to mechanical activation and that the low rate constants of chain scission were due to nonspecific cleavage along the polymer backbone. Collectively, these results suggested to us that mechanical forces were not inducing the formal [4 + 2] cycloreversion of the centrally located Diels−Alder adducts present within the $\mathbf{IV}_{Mn}$ materials.

To further demonstrate that the $\mathbf{IV}_{Mn}$ materials were not susceptible to mechanically facilitated cycloreversion, we polymerized methyl acrylate from an equimolar mixture of **III** and the known[2f] mechanically responsive congener **V** (Scheme 2). Pouring the corresponding reaction mixture into methanol (MeOH) resulted in the precipitation of a PMA material with an M_n = 79 kDa ($\mathbf{VI}_{79}$; Đ = 1.3). Dissolution of $\mathbf{VI}_{79}$ in acetonitrile (10 mg mL^{-1}) and subsequent ultrasonication afforded a new material that was isolated via precipitation from MeOH and filtration. GPC analysis of the isolated material revealed a bimodal distribution wherein a low molecular weight material was present (M_n = 38 kDa; Figure 4C). Moreover, ultraviolet−visible detection at 370 nm (a λ_{max} of anthracene) revealed that only the low molecular weight component exhibited a strong absorbance at this wavelength (Figure 4C). This result, in combination with the lack of mechanical reactivity that was observed for the $\mathbf{IV}_{Mn}$ materials, was

dx.doi.org/10.1021/ja4051108 | J. Am. Chem. Soc. 2013, 135, 12722−12729

consistent with the conclusion that polymers containing the previously reported mechanophore[2f] (i.e., those bearing polymer chains at the 9-position of the anthracene coupling partner) were undergoing mechanical cycloreversion to afford anthracenyl terminated polymer fragments.

To gain additional support for these results, we subjected $\mathbf{IV}_{88}$ to ultrasonication for 3 h as previously described (vide supra) and isolated the resulting material via precipitation from MeOH. Next, a tetrahydrofuran (THF) solution (10 mg mL^{-1}) of the postsonicated $\mathbf{IV}_{88}$ material was analyzed using ultraviolet−visible spectroscopy (Figure 4D). As expected, the characteristic absorbances of anthracene were not detected. Upon removal of the residual solvent, an equal mass of a polymer containing the previously reported[2f] mechanophore (M_n = 120 kDa; Đ = 1.4; $\mathbf{VII}_{120}$) was added, and the polymer mixture was dissolved in acetonitrile (10 mg mL^{-1}) and subjected to ultrasonication for an additional 3 h. The resulting material was isolated by precipitation from MeOH and dissolved in THF (10 mg mL^{-1}). Ultraviolet−visible spectroscopic analysis revealed characteristic absorbances associated with anthracene (Figure 4D). As such, we reasoned that while mechanical forces were capable of inducing formal [4 + 2] cycloreversions in materials comprised of the previously reported[2f] mechanophore, the newly designed analogue (i.e., the cycloadduct in $\mathbf{IV}_{Mn}$) did not undergo measurable mechanochemical activation, despite the similarity between the two systems. Taken together, these results were consistent with the theoretically predicted trends for the two sets of pulling points shown in Figure 3B. We note, however, that precise experimental measurements of the force dependencies of reaction rates (possibly via single-molecule pulling studies) would be required to experimentally quantify our theoretical predictions.

CONCLUSIONS

In sum, theoretical analysis revealed that anti-Hammond (rather than Hammond) behavior should be prevalent in the mechanically induced changes of molecular energy landscapes. In addition, our computational model predicted that mechanical forces may facilitate or suppress a given chemical transformation, depending on how they are applied. Experimental results supported the theoretically predicted reactivity trends and demonstrated that subtle changes in mechanophore design can lead to dramatic (and even counterintuitive) changes in mechanically induced reactivity. Moreover, the work reported here constitutes the first example of utilizing a theoretical model in the a priori design and development of a novel mechanophore. Beyond its fundamental importance, the ability to mechanically suppress chemical reactivity is expected to find applications in materials science (e.g., composites that resist mechanical degradation under stress) and facilitate future studies of force-induced biochemical phenomena.[20]

ASSOCIATED CONTENT

Supporting Information

Computational and experimental details, atomic coordinates, supplementary videos, and additional calculations. This material is available free of charge via the Internet at http://pubs.acs.org.

AUTHOR INFORMATION

Corresponding Author

makarov@cm.utexas.edu; bielawski@cm.utexas.edu

Author Contributions

§S.S.M.K. and J.N.B.: These authors contributed equally.

Notes

The authors declare no competing financial interest.

ACKNOWLEDGMENTS

We are grateful to Olga K. Dudko and John F. Stanton for comments. C.W.B., J.N.B., B.T.V., and K.M.W. were supported by the U.S. Army Research Office (W911NF-07-1-0409 and W911NF-11-1-0456) and the Robert A. Welch Foundation (F-0046). D.E.M. and S.S.M.K. were supported by the Welch foundation (F-1514) and the NSF (CHE 0848571). J.N.B. is grateful to the NSF for a predoctoral fellowship. D.E.M. acknowledges the W. A. "Tex" Moncrief, Jr., Endowment in Simulation-Based Engineering Sciences for a Grand Challenge Faculty Fellowship. Computational resources were provided by the Texas Advanced Computing Center.

REFERENCES

(1) (a) Caruso, M. M.; Davis, D. A.; Shen, Q.; Odom, S. A.; Sottos, N. R.; White, S. R.; Moore, J. S. *Chem. Rev.* **2009**, *109*, 5755. (b) Black, A. L.; Lenhardt, J. M.; Craig, S. L. *J. Mater. Chem.* **2011**, *21*, 1655. (c) Brantley, J. N.; Wiggins, K. M.; Bielawski, C. W. *Polym. Int.* **2012**, *62*, 2.

(2) (a) Hickenboth, C. R.; Moore, J. S.; White, S. R.; Sottos, N. R.; Baudry, J.; Wilson, S. R. *Nature* **2007**, *446*, 423. (b) Lenhardt, J. M.; Ong, M. T.; Choe, R.; Evenhuis, C. R.; Martinez, T. J.; Craig, S. L. *Science* **2010**, *329*, 1057. (c) Brantley, J. N.; Wiggins, K. M.; Bielawski, C. W. *Science* **2011**, *333*, 1606. (d) Wiggins, K. M.; Bielawski, C. W. *Angew. Chem., Int. Ed.* **2012**, *51*, 1640. (e) Brantley, J. N.; Konda, S. S. M.; Makarov, D. E.; Bielawski, C. W. *J. Am. Chem. Soc.* **2012**, *134*, 9882. (f) Wiggins, K. M.; Syrett, J. A.; Haddleton, D. M.; Bielawski, C. W. *J. Am. Chem. Soc.* **2011**, *133*, 7180. (g) Davis, D. A.; Hamilton, A.; Yang, J.; Cremar, L. D.; Van, G. D.; Potisek, S. L.; Ong, M. T.; Braun, P. V.; Martinez, T. J.; White, S. R.; Moore, J. S.; Sottos, N. R. *Nature* **2009**, *459*, 68.

(3) (a) Boulatov, R.; Kucharski, T. J. *J. Mater. Chem.* **2011**, *21*, 8237. (b) Ribas-Arino, J.; Shiga, M.; Marx, D. *Angew. Chem., Int. Ed.* **2009**, *48*, 4190. (c) Bailey, A.; Mosey, N. J. *J. Chem. Phys.* **2012**, *136*, 044102/1. (d) Konda, S. S. M.; Brantley, J. N.; Bielawski, C. W.; Makarov, D. E. *J. Chem. Phys.* **2011**, *135*, 164101. (e) Huang, Z.; Boulatov, R. *Pure App. Chem.* **2010**, *82*, 931. (f) Dopieralski, P.; Anjukandi, P.; Ruckert, M.; Shiga, M.; Ribas-Arino, J.; Marx, D. *J. Mater. Chem.* **2011**, *21*, 8309. (g) Ribas-Arino, J.; Marx, D. *Chem. Rev.* **2012**, *112*, 5412. (h) Kryger, M. J.; Munaretto, A. M.; Moore, J. S. *J. Am. Chem. Soc.* **2011**, *133*, 18992. (i) Franco, I.; Schatz, G. C.; Ratner, M. A. *J. Chem. Phys.* **2009**, *131*, 124902.

(4) (a) Bell, G. I. *Science* **1978**, *200*, 618. (b) Evans, E.; Ritchie, K. *Biophys. J.* **1997**, *72*, 1541. (c) Zhurkov, S. N. *Int. J. Frac. Mec.* **1965**, *1*, 311.

(5) (a) Suzuki, Y.; Dudko, O. K. *Phys. Rev. Lett.* **2010**, *104*, 048101. (b) Suzuki, Y.; Dudko, O. K. *J. Chem. Phys.* **2011**, *134*, 065102. (c) Dudko, O. K.; Graham, T. G.; Best, R, B. *Phys. Rev. Lett.* **2011**, *107*, 208301.

(6) Hyeon, C.; Thirumalai, D. *Biophys. J.* **2006**, *90*, 3410.

(7) (a) Tian, Y.; Boulatov, R. *ChemPhysChem* **2012**, *13*, 2277. (b) Tian, Y.; Boulatov, R. *Chem. Commun.* **2013**, *49*, 4187.

(8) Valiev, M.; Bylaska, E. J.; Govind, N.; Kowalski, K.; Straatsma, T. P.; Van Dam, H. J. J.; Wang, D.; Nieplocha, J.; Apra, E.; Windus, T. L.; de Jong, W. A. *Comput. Phys. Commun.* **2010**, *181*, 1477.

(9) Parr, R. G.; Yang, W. *Density-Functional Theory of Atoms and Molecules*; Oxford University Press: New York, 1989.

(10) Gordon, M. S.; Binkley, J. S.; Pople, J. A.; Pietro, I. W. J.; Hehre, W. J. *J. Am. Chem. Soc.* **1982**, *104*, 2797.

(11) (a) Becke, A. D. *J. Chem. Phys.* **1993**, *98*, 1372. (b) Zhao, Y.; Schultz, N.; Truhlar, D. G. *J. Chem. Theory Comput.* **2006**, *2*, 364.

(12) Gonzalez, C.; Schlegel, H. B. *J. Chem. Phys.* **1989**, *90*, 2154.

(13) Gonzalez, C.; Schlegel, H. B. *J. Phys. Chem.* **1990**, *94*, 5523.
(14) Marshall, B. T.; Long, M.; Piper, J. W.; Yago, T.; McEver, R. P.; Zhu, C. *Nature* **2003**, *423*, 190.
(15) (a) Barsegov, V.; Thirumalai, D. *Proc. Natl Acad. Sci. USA* **2005**, *102*, 1835. (b) Prezhdo, O. V.; Pereverzev, Y. V. *Acc. Chem. Res.* **2009**, *42*, 693.
(16) Li, H.; Cao, Y. *Acc. Chem. Res.* **2010**, *43*, 1331.
(17) (a) Akbulatov, S.; Tian, Y.; Kapustin, E.; Boulatov, R. *Angew. Chem., Intl. Ed.* **2013**, *52*, 6992. (b) Dopieralski, P.; Ribas-Arino, J.; Anjukandi, P.; Krupicka, M.; Kiss, J.; Marx, D. *Nat. Chem.* **2013**, DOI: 10.1038/nchem.1676.
(18) Browne, W. R.; Feringa, B. L. *Nat. Nano.* **2006**, *1*, 1748.
(19) (a) Voth, G. A.; Hochstrasser, R. M. *J. Phys. Chem.* **1996**, *100*, 13034. (b) Hanggi, P.; Talkner, P.; Borkovec, M. *Rev. Mod. Phys.* **1990**, *62*, 251.
(20) Makarov, D. E. In *Single-molecule Studies of Proteins*; Oberhauser, A. F., Ed.; Springer: New York, 2013.
(21) Jagannathan, B.; Elms, P. J.; Bustamante, C.; Marqusee, S. *Proc. Natl Acad. Sci. USA* **2012**, *109*, 17820.
(22) (a) Mantovani, G.; Lecolley, F.; Tao, L.; Haddleton, D. M.; Clerx, J.; Cornelissen, J. J. L. M.; Velonia, K. *J. Am. Chem. Soc.* **2004**, *127*, 2966. (b) Percec, V.; Guliashvili, T.; Ladislaw, J. S.; Wistrand, A.; Stjerndahl, A.; Sienkowska, M. J.; Monteiro, M. J.; Sahoo, S. *J. Am. Chem. Soc.* **2006**, *128*, 14156−14165.
(23) Anthracene was not observed after heating a 10 mg mL^{-1} solution of $\mathbf{IV}_{88}$ to 130 °C for 19 h.